



HAL
open science

Bioresorbable polylactic acid (PLA) and bioactive glasses (BG) composite: influence of gold coated of BG powder on mechanical properties and chemical reactivity

Louis Chaigneau, Aurélien Perrot, Damien Brézulier, Jean-François Coulon, François Cheviré, Ronan Lebullenger

► To cite this version:

Louis Chaigneau, Aurélien Perrot, Damien Brézulier, Jean-François Coulon, François Cheviré, et al.. Bioresorbable polylactic acid (PLA) and bioactive glasses (BG) composite: influence of gold coated of BG powder on mechanical properties and chemical reactivity. *Journal of the mechanical behavior of biomedical materials*, 2023, 10.1016/j.jmbbm.2022.105571 . hal-03852711

HAL Id: hal-03852711

<https://univ-rennes.hal.science/hal-03852711>

Submitted on 21 Nov 2022

HAL is a multi-disciplinary open access archive for the deposit and dissemination of scientific research documents, whether they are published or not. The documents may come from teaching and research institutions in France or abroad, or from public or private research centers.

L'archive ouverte pluridisciplinaire **HAL**, est destinée au dépôt et à la diffusion de documents scientifiques de niveau recherche, publiés ou non, émanant des établissements d'enseignement et de recherche français ou étrangers, des laboratoires publics ou privés.

Title: Bioresorbable polylactic acid (PLA) and bioactive glasses (BG) composite: influence of gold coated of BG powder on mechanical properties and chemical reactivity

Auteurs :

- Louis CHAIGNEAU : Univ Rennes 1, CNRS, ISCR (Institut des Sciences Chimiques de Rennes), UMR 6226, F-35000, Rennes, louis.chaigneau@univ-rennes1.fr
- Aurélien PERROT : ECAM Rennes - Louis de Broglie, Campus de Ker Lann – 35170 Bruz, France. Univ Rennes 1, CNRS, ISCR (Institut des Sciences Chimiques de Rennes), UMR 6226, F-35000, Rennes. aurelien.perrot@cea.fr
- Damien BRÉZULIER : Univ Rennes 1, CNRS, ISCR (Institut des Sciences Chimiques de Rennes), UMR 6226, F-35000, Rennes, damien.brezulier@univ-rennes1.fr
- Jean-François COULON, ECAM Rennes - Louis de Broglie, Campus de Ker Lann – 35170 Bruz, France. jean-francois.coulon@ecam-rennes.fr
- François CHEVIRÉ : Univ Rennes 1, CNRS, ISCR (Institut des Sciences Chimiques de Rennes), UMR 6226, F-35000, Rennes. francois.chevire@univ-rennes1.fr
- Ronan LEBULLENGER : Univ Rennes 1, CNRS, ISCR (Institut des Sciences Chimiques de Rennes), UMR 6226, F-35000, Rennes. ronan.lebullenger@univ-rennes1.fr

Abstract :

Due to the ageing of the population, the synthesis of biomaterials and the optimization of their physico-chemical characteristics are at the heart of many research projects in regenerative medicine. The emergence of 3D printing techniques has rapidly led to the manufacture PLA-BG composite scaffolds using the FFF (Fused Filament Fabrication) technic. However, this composite presents some problems including a lower mechanical strength than the two compounds alone, probably due to the ionic salting-out induced by the BG. This study aims to counter this phenomenon by coating the BG particles with a thin layer of gold. The 3D composite objects will then be characterized mechanically and biologically to ensure that the bioactive character of the composite is preserved.

Keywords: polylactic acid, bone tissue engineering, composite materials, Polymer-ceramic composite; Bioactivity; Degradable polymers; Bioactive glass; mechanical properties

Abbreviations

Bioactive glass(es): BG

Fused filament fabrication: FFF

Poly-lactic acid: PLA

Computer Aided Design and Manufacturing: CAD/CAM

Size exclusion chromatography: SEC

Simulated body fluid: SBF

1. Introduction

The world of biomaterials has progressed tremendously in recent years. Biocompatibility is no longer a sufficient requirement and now these materials must exhibit a bioactive character. This means that they should induce a specific biological response involving surface reactions thus leading to the creation of intimate bonding at the interface with the host tissue.

Bioactive glasses (BG) include different compositions of synthetic inorganic amorphous silica-based materials. The first bioactive glass, Bioglass 45S5[®], was discovered in 1969 by Larry Hench [1]. Since then, several other formulations have been reported [2] and a silica content lower than 60 wt% appears to be the requirement for sufficient bioactivity [3]. The chemical reactivity of BG is usually demonstrated by the formation of a hydroxyapatite layer on the surface of the material upon prolonged contact with a simulated body fluid (SBF).

Poly-lactic acid (PLA) is a biodegradable polyester obtained by polymerization of lactic acid itself made by fermentation of sugars derived from renewable resources [4] such as corn starch that is considered an environmentally friendly thermoplastic polymer [5]. The United States of America Food and Drug Administration approved its use in contact with human biological fluids in 1970. Consequently, due to its biocompatibility and degradability in the human body, PLA has been adopted in various medical applications such as interference screws for the hand, ankle and knee [6] or surgical threads [7]. Upon contact with body fluids, PLA undergoes a hydrolytic degradation into lactic acid that can be then eliminated by the body as CO₂ and H₂O [8].

As both BG and PLA are biocompatible materials, a fruitful research has been carried out to combine them. The suitability of such composite as a scaffold for bone replacement has been investigated on various biological tests: bioactivity, in vitro degradation, ... [9] [10] [11] [12] [13]. The PLA/BG composite exhibits the specific properties of both the polymer and the BG; The thermoplastic matrix is radiolucent and bioresorbable while the BG promotes osteosynthesis, stimulates angiogenesis and accelerates osteosynthesis.

Prior to the late 2000s and the emergence of additive manufacturing, the use of composites as orthopaedic biomaterials was very limited, mainly due to issues associated with their design and manufacture [14]. Tissue engineering has therefore recently focused on the production of composites by additive manufacturing, allowing the creation of objects with complex shapes and geometries through the use of CAD/CAM (Computer Aided Design and Manufacturing) software. The most common processes are extrusion, photopolymerization, powder bed fusion and material jetting. P. Stavropoulos and P. Foteinopoulos have recently listed and classified the additive manufacturing techniques [15].

The FFF (Fused Filament Fabrication) approach is based on the extrusion of a fusible filament and its deposition layer by layer using a printing nozzle driven by a 3-axis system. Once a layer is completed, the scaffolding under construction is vertically offset to allow the next layer to be extruded, until the final object is obtained. The layer thickness determines the quality of the 3D printing with resolution usually between 50 and 200 μm [16].

Regarding biomedical experiments, PCL (polycaprolactone), PLGA (poly(lactic-co-glycolic acid)), PLA (polylactic acid) and their combination with other biomaterials are among the preferred alternatives to produce scaffolds by FFF [17]. PLA is one of the most widely used polymers for biomedical and general applications [18], due to its low temperature extrusion which is between 190 and 230°C [19] thus allowing the use of low cost printers [20]. However, it is essential to control the extrusion mechanism so that PLA is not exposed to excessive shear stresses, which could subsequently affect its biocompatibility and cause its degradation. Using size exclusion chromatography (SEC), Grémare et al have shown the possibility of a drop-in polymer chain size from 100 to 54 kDa using the FFF process [21].

Yet, the mechanical properties of a polymer composite, which derived from the polymer chain size, are essential in the orthopaedic field to withstand the stresses exerted on the implant. Engelberg et al. showed that a doubling of the mass average chain size of PLA from \bar{M}_w of 50,000 to 100,000 g.mol⁻¹ doubled its tensile strength [22]. For PLA/Bioglass 45S5[®] composites, N. Ginsac demonstrated that their mechanical strength was lower than the polymer or Bioglass 45S5[®] alone [23], as a result of degradation of the polymer chain by ionic species released from the BG on the PLA.

Therefore, the objective of this study is to reduce this phenomenon by coating the BG with a thin layer of gold by sputtering to limit its ionic release into the polymer. Although gold is sometimes associated with a cytotoxic metal, it is actually used in many medical applications [24]. Its remarkable physico-chemical properties, including biocompatibility, are mostly induced by the size, charge and shape of the gold particles used [24] [25]. It is important to note that the focus of this study is on the mechanical properties of the composite and not on in vitro cellular testing. Indeed, the nano-size of the deposited gold particles necessarily leads to cell death [26]. This new cathodic sputtering method allows a simple and inexpensive first approach in the laboratory.

2. Materials and methods

a. Manufacture of the PLA-bioactive glass (BG)_Au composite

Raw materials: The PLA powder used for the experiments is the RXP 7501 PLA from Resinex with a mechanical strength of 48 MPa and a density of 1.240 according to the manufacturer's specs. The 40-70 μm soda-lime silicate glass beads come from Hd Tooling and have the following overall composition (SiO₂: 70.00 - 75.00 wt.%; Na₂O: 12.00 - 15.00 wt.%; CaO: 7.00 - 12.00 wt.%; MgO: max. 5.00 wt.%; Al₂O₃: max. 2.50 wt.%; K₂O: max. 1.50 wt.%; Fe₂O₃: max. wt.0.50 %). Raw precursors for 45S5[®] BG (BG) synthesis are SiO₂ from Quartz et Silice (99,9% purity), Na₂CO₃ from Acros Organics (99.5% purity), CaCO₃ from Alfa Aesar (99,0% purity) and NaH₂PO₄ from Acros Organics (99+% purity).

The synthesis of bioactive glass is a multistep process. First, the starting materials are weighed, mixed and crushed in an agate bowl. The mixture is then heated up to 850°C for 90 minutes in a platinum crucible, placed in a muffle furnace and dwelled for 20 minutes to allow decarbonation. Finally, the mixture is heated at 1350°C for 45 minutes to reach the melting and fining step. The resulting liquid is poured onto a stainless-steel support and then cooled in ambient laboratory atmosphere. The BG is then ground using a mechanical grinder with an agate bowl. The resulting powder is finally sieved to a particle size smaller than 100 μm and checked by laser granulometry measurements. The polymer/glass composite precursor is then obtained by mixing the as-prepared glass powder with the PLA Resinex powder using a turbula until a homogeneous mixture is obtained.

Gold coating by sputtering: Gold deposition is achieved by sputtering with a Leica plasma sputterer under Argon with a gold target. The BG, previously reduced to powder, is placed on a support and spread to form a monolayer. A high vacuum operation is applied followed by diffusion metallization for 150 seconds. The resulting metallized powder is then mixed with a spatula and the process is repeated three times to obtain a powder with a thin layer of gold. As this process does not provide a perfect gold coating on the BG powder, the attack of organic liquids on the BG is partially retained, allowing the chemical reactivity of the composite.

Setting up filament production: Composite filaments were fabricated using a Noztech Touch extruder equipped with a hopper, an auger and a 1.75mm nozzle paired with a lab-made monitored spooler. A fine control of the extrusion flow and the winding speed allowed to obtain composite filaments with a homogenous diameter of $1.75 \pm 0.05\text{mm}$.

Object design: The 3D specimens for mechanical characterizations and 3D parts for SBF tests are first modelled using the open-source software FreeCAD [27]. The 3D file is then converted to a tessellation STL file that can be fed to the slicer software, here the Cura software [28]. The CNC programming language (G-code) for the 3D printer is obtained using the following parameters: 100% gyroid filling, 150 μm layer height, 50 °C bed temperature and 200 °C for the printing head. The printer used is a Prusa i3 modified RepRap-style 3D printer based on Anet A8 parts equipped with a 1mm nozzle in order to avoid clogging during extrusion of the glass particles charged PLA.

Tensile tests: Tensile tests are performed using the Instron 3369 tensile testing machine and an extensometer. The specimens used are according to the ISO -527-2 (5A standard). The working speed is 1 mm/min. The positioning of the specimen is checked to ensure that the specimen is straight. At the start of each test, a calibration is carried out and the extensometer is removed at Rp0.2. Groups of 5 specimens are taken for each parameter to obtain an average and to observe the variability of the measurements.

SEM: To observe the topology and determine the qualitative composition of the resulting 3D pieces, two SEMs were used at room temperature: the JEOL JSM 7100 F and the JEOL IT 500 HR, all coupled to an EDS unit. The images were taken at a voltage varying between 5 and 15keV. When necessary, the samples were metallized with carbon using a Leica plasma metallizer sputter.

Optical microscopy: For optical imaging, a Keyence VHX-7000 series digital optical microscope was used. It allows 2D and 3D digital modelling of samples with a magnification range of x100 to x1000 and a maximum resolution: 4800 x 3600.

b. Gold coating effects on the polymer chains of PLA–BG composite

Size Exclusion Chromatography: Weight average molar mass (M_w) and dispersity ($\bar{D} = M_w/M_n$) values were measured by size exclusion chromatography (SEC) in tetrahydrofuran (THF) at 40 °C (flow rate = 1.0 mL/min) on a GPC2502 Viscotek apparatus equipped with a refractive index detector Viscotek VE 3580 RI, a guard column Viscotek TGuard, Org 10 x 4.6 mm, a LT5000L gel column (for samples soluble in organic medium) 300 x 7.8 mm and a GPC/SEC OmniSEC Software [29]. The polymer samples were dissolved in THF (2 mg/mL). All elution curves were calibrated with polystyrene standards.

c. Characterization of Ca – P layer and solution ion concentration

XRD: Structural determination of the compounds was performed by X-ray diffraction (XRD) using a Panalytical X' Pert Pro" diffractometer (Cu-L2, L3 radiation, $\lambda = 1.5418 \text{ \AA}$, 40 kV, 40 mA, PIXcel 1D detector). They were collected at room temperature in the 2θ range 5-120° with a step size of 0.0131° and a scan time per step of 200 s. Data Collector and HighScore Plus software were used for data recording and analysis.

FTIR-ATR: Attenuated Total Reflection Fourier Transform Infrared spectra were recorded at room temperature using a Bruker Equinox 55 FTIR spectrophotometer, continuously purged with air. Opus software (4.2.37) [30].

ICP-OES: Chemical analyses on P, Si and Ca elements concentrations in the SBF solution containing composites were performed using an iCAP 7000 series optical plasma emission spectroscopy (ThermoFischer Scientific). The wavelengths studied for the elements Si, Ca and P are available in Annexes. A calibration curve was performed with control samples framing the concentration range. The analysed samples were dissolved in 2% fluoride acid before being inserted into the nebulizer [31].

SBF (Simulated Body Fluid) preparation: For the SBF realization, two calcium and phosphorus rich ionic solutions were prepared at 37°C under stirring. For the first solution, 50mM tris(hydroxymethyl)aminoethane, 5 mM CaCl_2 and 3 mM $\text{MgCl}_2 \cdot 6\text{H}_2\text{O}$ were introduced into a 1L volumetric flask, supplemented with distilled water. For the second solution, 50mM tris(hydroxymethyl)aminomethane, 2 mM K_2HPO_4 , 8.4 mM NaHCO_3 , 6 mM KCl and 275.6 mM NaCl were inserted into another 1 L volumetric flask, also completed with distilled water. The pH of these solutions was then adjusted to 7.4 with 6N HCl. Finally, to obtain the SBF, the two solutions were mixed with a 50-50 volume ratio [32].

The solid samples were made from used tensile specimens with dimensions of 12.5 mm side and 2 mm thickness. Their surface area was 4.12 cm² and the ratio of sample surface area to SBF volume of the sample was 6.86.10⁻² cm⁻¹. The surfaces were polished with abrasive paper FEPA 4000 (5µm). The samples were then cleaned with distilled water and ethanol, dried with an air compressor and placed in a desiccator for 24 hours. They were then immersed in 60 mL of SBF and placed in an incubator at 37 °C under agitation at 60 rpm for the desired time. A control group consisting exclusively of SBF was also carried out. The immersion times were 3, 14, 28 and 57 days. Once removed from the SBF, the samples were rinsed with ethanol and distilled water and then placed in an oven at 50°C for 24 hours, followed by 48 hours in a desiccator.

3. Results and discussion

a. Characterization of printed polymer composites

In order to observe the adhesion of the gold particles to the BG during the metallization sputtering process, Keyence optical microscopy images were taken of metallized glass beads (for better visualization) as well as of non-metallized beads. The behaviour observed for glass beads is identical to that observed for bioactive glass powders. These shots are shown in [Figure 1](#). A difference in color is well observed between the metallized and non-metallized beads demonstrating good adhesion of the gold particles to the glass. However, the colors are not uniform with darker or lighter shades. This is due to an imperfect homogenization of the gold deposit on all the glass beads. This observation does not necessarily have any consequence on this study. Indeed, the objective is to allow the growth of the hydroxyapatite on the surface of the BG and too much gold could alter its development.

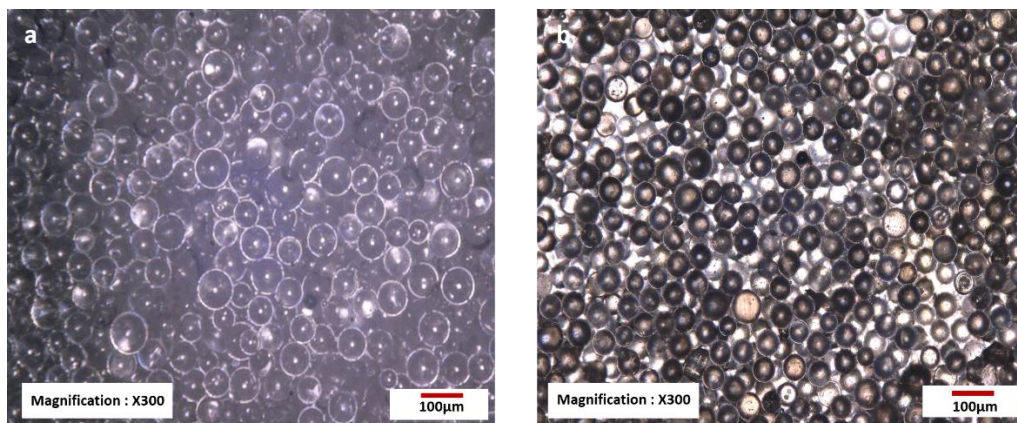


Figure 1 : Glass beads: a. Non-metallized beads at 300x magnification; b. Metallized beads at 300x magnification

Once the production of the composite filaments (1.75 mm diameter) is achieved, we checked the homogeneity of the distribution of the mineral fillers into the PLA matrix. A digital analysis by image processing was carried out using a SEM image of a longitudinal section (1.20*0.8mm) of a PLA (70%wt)/BG (30%wt) filament. A Python program and the Scikit-image library were used for this purpose. The image was converted into a PGM format and then binarized into black and white by choosing a suitable threshold. The white and black pixels were then counted and the percentage of white pixels was calculated. The experimental result shows a volume fraction of 18% in BG while the calculus gives 17.6%. The results are therefore consistent and confirm the good homogeneity of the distribution of mineral particles in the polymer matrix.

In order to verify the presence or persistence of the gold coating on the BG particles once inserted in PLA, a secondary electron SEM picture and an EDS analysis were carried out on the same area and their superposition is presented in [figure 2.a](#). A concentration of gold is observed (orange spots) around the BG grains confirming the good adhesion of the gold on the BG and its resistance to the two extrusion steps (filament production and FFF 3D print). Optically, we observe on the [figures 2.b and 2.c](#), a differentiation of colors for the specimens whose BG underwent a metallization. They have completely blackened due to the diffusion of light by gold in the composite. On the other hand, the specimens blackened homogeneously over the entire material, again indicating good dispersion.

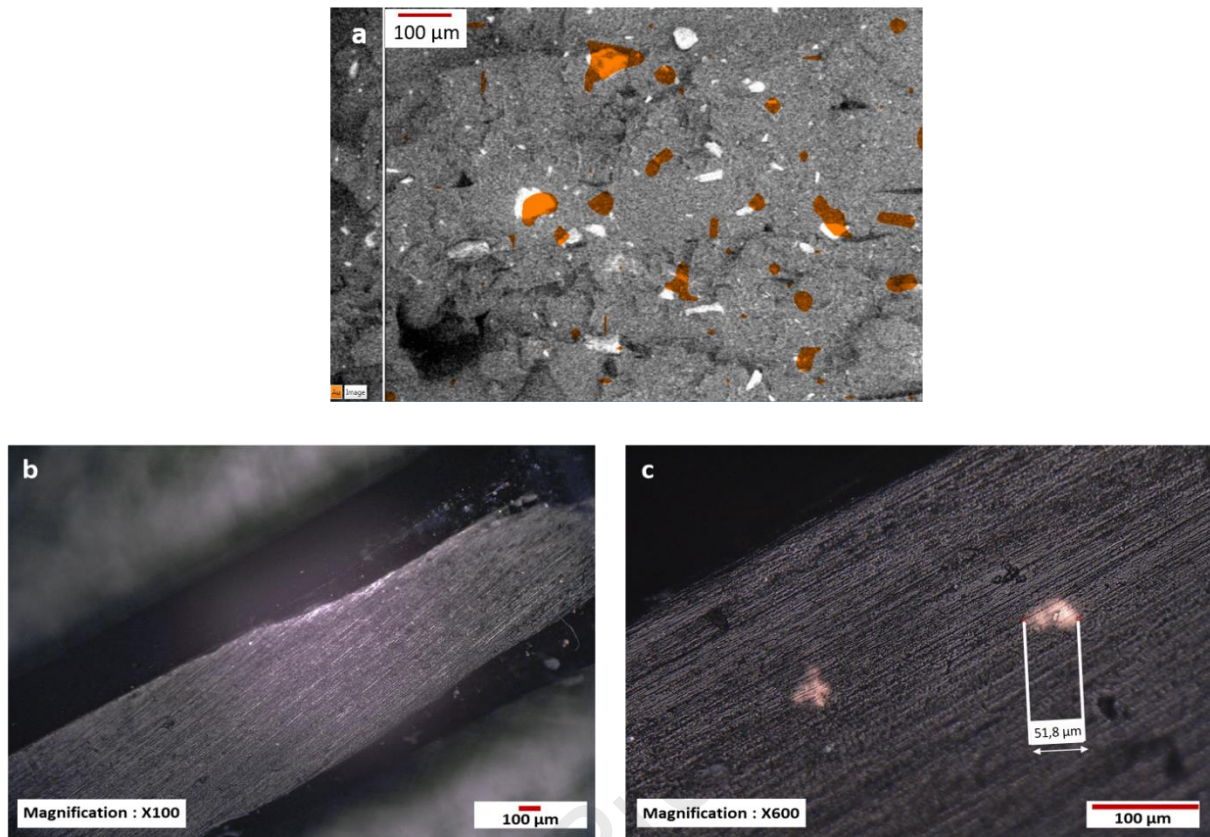


Figure 2 : Microscopic analysis of a metallized PLA/BG composite filament: a. Superposition of a SEM image and gold presence map (orange spots); b. Keyence shot of the sample at 100x magnification; c. Keyence shot of the sample at 300x magnification

b. Gold coating effects on the mechanical properties of PLA–BG composite

Table 1 : Composition (wt. %) of the 3D FFF printed samples used for the mechanical tests

	wt. % PLA		wt. % glass		Gold coating by sputtering
	Commercial powder (Resinex)	Soda lime silica glass beads	Soda lime silica glass powder	BG powder (45S5® BG)	
#1	100		0		
#2	90	10			
#3	70	30			
#4	90		10		
#5	90			10	
#6	90			10	X

When composites are used as bone substitutes, the study of their mechanical characteristics is necessary. The final construction must necessarily approximate the physico-chemical properties of the tissue to be regenerated in order to maintain the functionality of the tissue [33]. In our study, six groups of mechanical specimens were printed by FFF technic in the laboratory, in order to understand the influence of the structural conditions of the composites on their mechanical properties. Their compositions are presented in [Table 1](#). The influence of the mass fraction, shape, composition and metallization of the mineral filler in the polymer matrix was studied.

According to [Figure 3](#), all the produced composites presented a tensile strength curve typical of a ductile fracture except for the untreated PLA/BG composite (green curve #5). They are representative of plastic materials because they present a linear part, a yielding point, a hardening and a necking phases. Indeed, they all showed the ability to deform plastically without breaking until the first defect appeared. The five tested mechanical PLA/BG specimens, on the other hand, fractured as soon as their elastic limit was reached. SEM images of the fracture surfaces of the specimens were taken to illustrate this hypothesis. Those of the PLA/BG (#5) and PLA/Gold-metallized BG (#6) composites are shown in [Figure 4.b and 4.c](#). A typical brittle fracture surface is observed for the composite with untreated BG, whereas a ductile fracture is obtained for the composite with gold-coated BG particles. The results are therefore concordant.

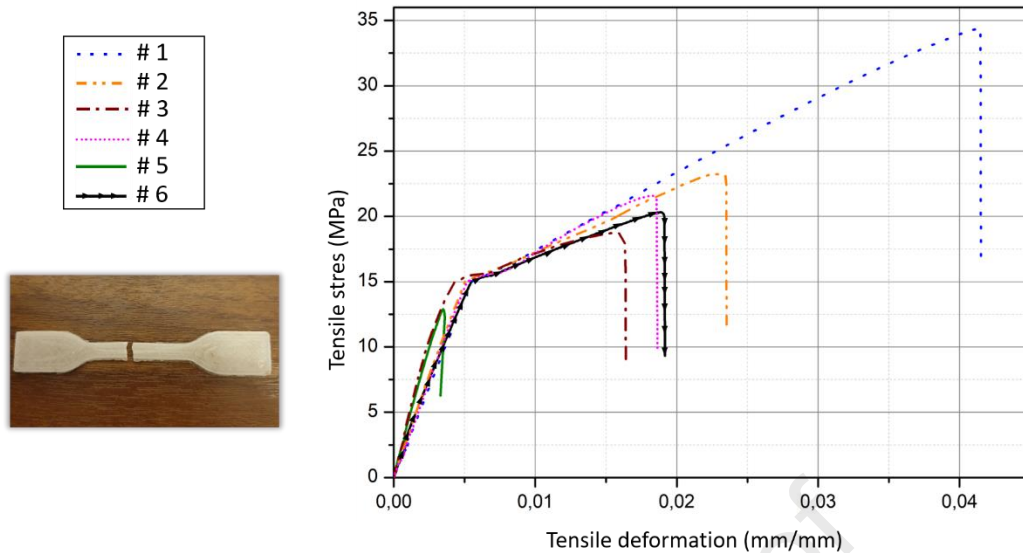


Figure 3 : Typical stress-strain curves of the different composites

Figure 4.a shows the maximum mechanical strength of the different produced composites. Firstly, the mechanical strength of the extruded pure PLA (39 MPa) has decreased by 9 MPa compared to that given by the supplier (48 MPa). This is probably partly due to the shear stresses experienced during extrusion. However, it was still in agreement with the values found in the literature [34].

When looking at the variation of the mineral filler fraction in the composite, it was observed that the composite (#3) with 30wt% glass bead filler had a lower maximum strength (16 MPa) than the composite (#2) with only 10wt% glass bead filler (26 MPa). This result demonstrates the importance of minimizing the mineral reinforcement content in PLA matrices to maximize its tensile strength.

In addition, the shape of the mineral filler inserted into the matrix also seems to be a determining factor. For the same weight glass fraction, the composite (#2) with glass beads (isotropic particles) shows a higher maximum mechanical strength (26 MPa) than the composite (#4) with glass powder (18 MPa). The sharp corners of the powder particles certainly degraded the PLA polymer chains and promoted shear by stress concentration.

When designing high-strength PLA-glass composites, it therefore seems wise to control the extrusion parameters and to use glass reinforcement in the form of beads and with the lowest possible mass fraction.

However, the chemical composition of the mineral filler also has a significant effect on the mechanical tensile properties of the composites. The use of BG, with a chemical composition closed to 45S5[®], as a mineral filler alters the ion exchange at the interface between the PLA matrix and the glass reinforcement. The high contents of Ca, Na and the presence of P decreases the maximum mechanical strength (9 MPa) when compared to a conventional glass composition (18MPa). In addition, the gold metallization of the BG particles also leads to a change in the interface between the BG grains and the PLA matrix. The mechanical properties of the composite including the glass metallized with gold (#6) are close to those of the composite including the soda lime silicate glass (#4). This seems to have a positive effect as an enhance in the maximum mechanical strength is observed (19 MPa).

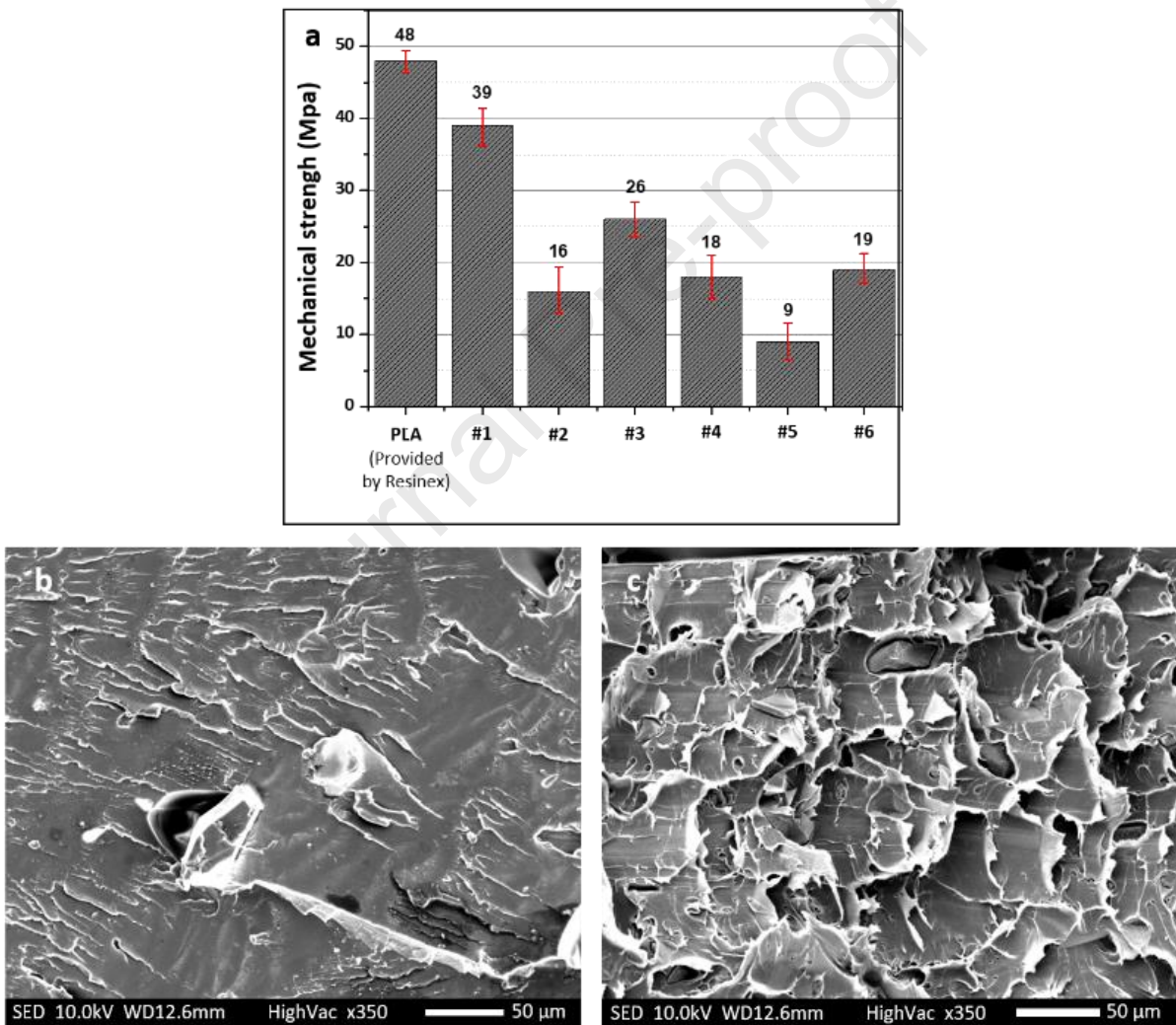


Figure 4 : (a) Maximum mechanical strength of composites; (b) SEM image of brittle fracture surface of PLA/BG (#5); (c) SEM image of ductile fracture surface of PLA/BG metallized with gold (#6)

In order to interpret these results, size exclusion chromatography (SEC) measurements were carried out. These analyses made it possible to determine the number and mass average molecular weight of the PLA chains for the different composites. SEC results are shown in [Figure 5](#). Once extruded, the PLA chains have a number and mass average molecular mass of approximately $M_n = 53,000 \text{ g.mol}^{-1}$ and $M_w = 120,000 \text{ g.mol}^{-1}$. When 10wt% BG powder was added, the size of the polymer chains decreased by about 2 ($M_n = 28,000 \text{ g.mol}^{-1}$ and $M_w = 65,000 \text{ g.mol}^{-1}$). Several properties can be blamed. Firstly, for the same reasons as mentioned above, the fact that the BG in crushed powder form leads to cleavage of certain PLA chains. Secondly, the increase in Na content compared to conventional glass increases the formation of a basic catalysis and therefore the hydrolysis of the PLA chains, thus reducing the molecular weight of the polymer and its mechanical strength [21]. Gold metallization of BG seems to limit this last phenomenon. The number and mass average molecular weight for the treated BG increased compared to the untreated compound ($M_n = 36,000 \text{ g.mol}^{-1}$ and $M_w = 81,000 \text{ g.mol}^{-1}$). As gold is theoretically located at the interface between PLA and BG, it seems to restrict the release of Na^+ ion and therefore restrict the hydrolysis of the polymer chains, allowing an enhance for mechanical strength.

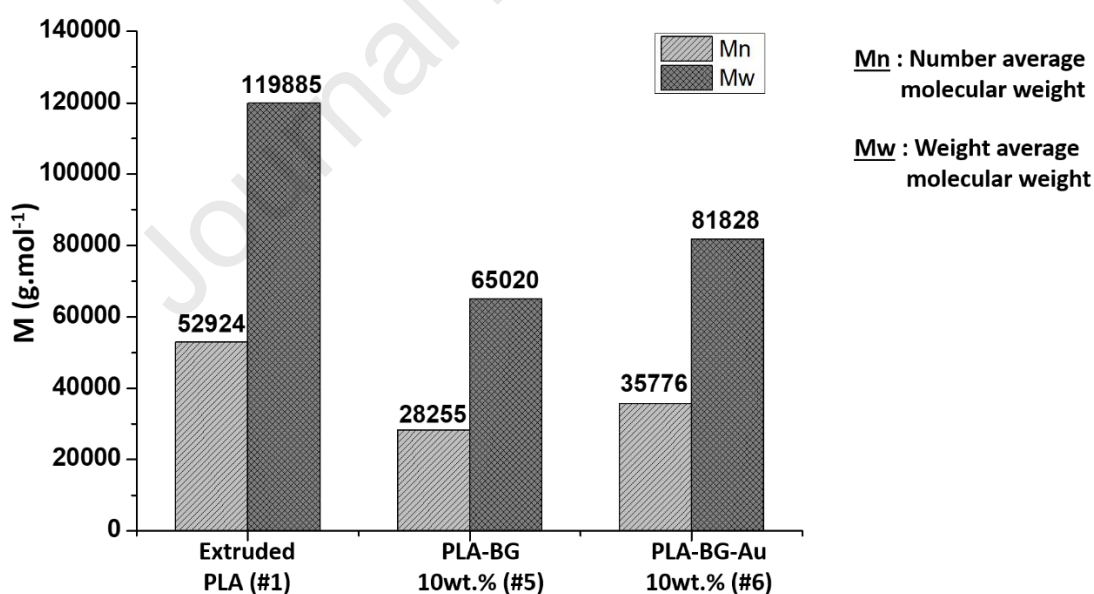


Figure 5 : Number and weight average molecular weight of extruded PLA (#1), PLA/BG (#5) and PLA/ BG metallized with gold (#6)

c. Gold coating effects on chemical reactivity of PLA-BG composite

The chemical reactivity of a biomaterial is traditionally associated with the mechanism of hydroxyapatite formation after immersion of samples in a biological medium. Hydroxyapatite, a mineral species and the main component of tooth enamel, dentin and bone, can significantly affect cell viability and proliferation [35]. Generally, *in vitro* tests in biological fluids are performed before *in vivo* tests to ensure the formation of hydroxyapatite. In SBF, the thickness of the hydroxyapatite layers increases with immersion time [36]. The layers consist mainly of silica, but hydroxyapatite and a mixed layer of silica and hydroxyapatite are formed during prolonged immersion. In *in vivo* experiments, the formation of hydroxyapatite follows the same pattern as *in vitro*. However, *in vivo*, the layers are more diffuse and mixed layers of silica and hydroxyapatite appear. PK. Vallittu et al. showed that after 5 months of implantation of bioactive glasses into calvarial defects, the formation of viable, non-inflammatory mesenchymal tissue with newly formed mineralised woven bone was observed, as well as non-mineralised connective tissue with larger capillaries and blood vessels. The presence of osteocytes was also detected in the newly generated bone matrix [37].

The approach used here to determine the chemical reactivity is an immersion in SBF of the composites with immersion times of 0, 7, 14, 28 and 57 days. The tests were carried out on a pure PLA structure, a PLA-BG composite, a PLA-BG metallized with gold composite and a control solution containing only SBF.

ICP AES allows the measurement of ionic concentration of an aqueous solution with a high degree of accuracy (uncertainty of 1 ppm). In this work, it allows us to observe the ionic exchanges that take place between the SBF and the different compounds over time. The results obtained are presented in [Figure 6.a, b. and c.](#) They show, as expected, almost no variation in Si, P and Ca concentrations after 57 days for the control test and the SBF containing only pure PLA (red disk on graphs). However, for the composites containing a mineral filler, an increase in Si concentration and a decrease in P and Ca are observed. The increase in Si concentration can be attributed to the partial dissolution of the glass in the SBF. This dissolution not being congruent, it allows the formation of a layer of silica gel on the surface of the partially dissolved BG grains. Crystals of calcium phosphates can then grow on this gel layer [38]. Furthermore, for these three elements, the increase in Si concentration and the decrease in Ca and P were limited for the composite where the BG underwent metallization compared to that which did not receive any coating treatment. The gold metallization of the BG grains therefore moderates the chemical reactivity of the compound. It should be noted that no gold concentration was detected for the metallized compound even after 57 days of immersion in SBF.

The decrease in Ca and P therefore suggests the transformation of these trace elements into calcite or even hydroxyapatite. To verify this hypothesis, SEM images of the two composites were taken after 57 days of immersion. They are presented in [figure 7](#). On the surface of the sample, numerous hydroxyapatite clusters were observed for both composites. They were easily identifiable as they were all located in cracks in the composite caused by the mechanical stresses experienced by the compounds. Numerous spheres stuck together were observed with hydroxyapatite crystals developing on their surface. These observations are only qualitative and do not allow for a quantification of the hydroxyapatite in the samples. However, from the ICP AES study, it appears that the hydroxyapatite layer appears to grow more prominently for the unmetallized bioglass (#5) because gold metallization reduces ionic releasing, the main factor influencing hydroxyapatite formation.

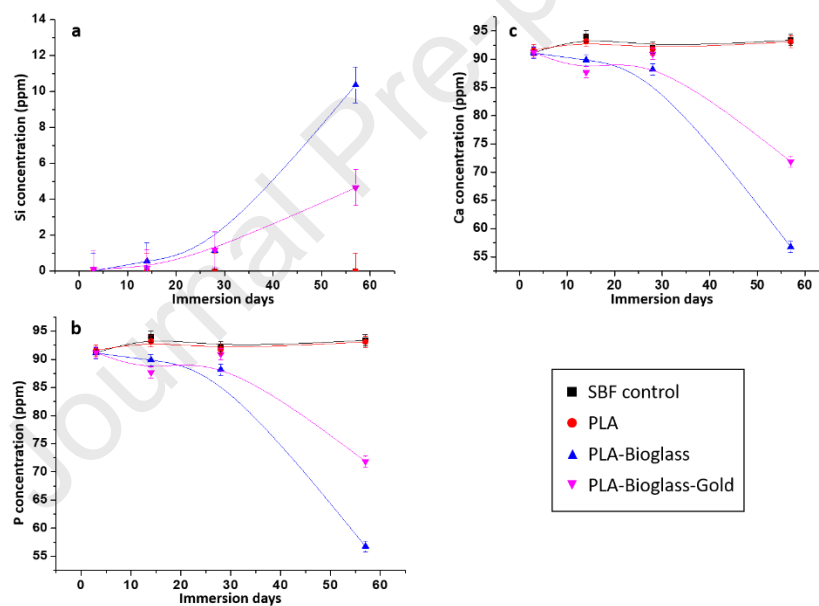


Figure 6 : ICP measurements to determine the concentration of the elements (a) Si; (b) P and (c) Ca of the composites after immersion in SBF for 0, 7, 14, 28 and 57 days

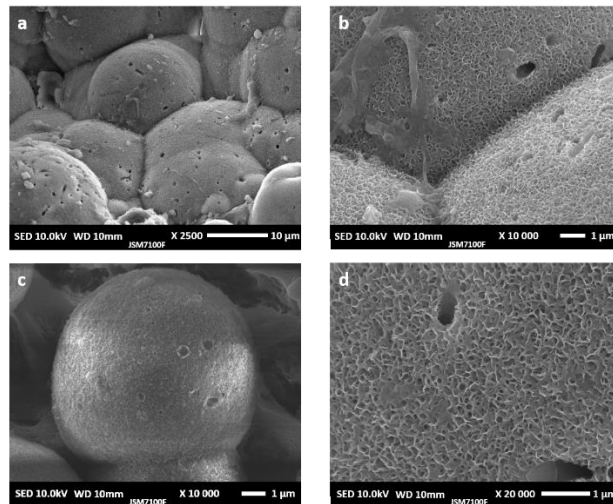


Figure 7 : SEM images of (a) (c)PLA/BG and (b) (d) PLA/BG metallized with gold composites

4. Conclusion

Mechanical specimens of PLA/glass or PLA/BG composites were successfully prepared by FFF 3D printing. For gold metallization, Keyence images showed that the gold particles adhered well to the BG but not homogeneously. However, the production of the printing filaments as well as the printed parts showed a good distribution of the mineral fillers within the polymer matrix.

The mechanical tests showed that the mechanical properties of the composites depend on several physical factors including the fraction of mineral filler inserted in the matrix and its shape. The composition of the mineral filler is also an important factor because the substitution of glass beads by BG resulted in a strong decrease in the tensile strength due to the degradation of PLA chains by the ionic release of BG. On the other hand, the presence of gold particles at the PLA-BG interface limited ionic releasing and therefore maximized the mechanical tensile properties. The addition of gold appeared to slightly reduce the kinetics of hydroxyapatite formation in contact with SBF but did not inhibit it. The present work suggests that the insertion of gold particles on the BG surface in a PLA-BG composite can enhance its mechanical properties without irreversibly affecting its chemical reactivity.

5. Acknowledgment

The authors wish to thank Sandrine Cammas-Marion (ISCR – ENSCR) for her technical assistance during the SEC, as well as Bertrand Lefeuvre for his technical assistance during the ICP-AES.

This publication is supported by the European Union through the European Regional Development Fund (ERDF), the Ministry of Higher Education and Research, the French Region of Brittany and Rennes Métropole.

6. CRediT

Louis Chaigneau: Conceptualization, Methodology, Validation, Investigation, Data Curation, Writing - Original Draft, Writing - Review & Editing,

Aurélien Perrot: Conceptualization, Methodology, Formal analysis, Software, Writing - Original Draft, Visualization.

Damien Brézulier: Methodology,

Jean-François Coulon: Funding acquisition

François Cheviré: Methodology, Writing - Review & Editing, Supervision

Ronan Lebullenger: Conceptualization, Funding acquisition, Methodology, Writing - Review & Editing, Supervision.

7. Annexes

Dosing element	Wavelengths (nm)						
P	177.495	178.284	178.766	185.891	185.942	213.618	214.914
	(Axial /Radial)	(Axial /Radial)	(Axial /Radial)	(Axial /Radial)	(Axial /Radial)	(Axial/Radial)	(Axial /Radial)
Si	212.412	251.611					
	(Axial /Radial)	(Axial /Radial)					
Ca	184.006	317.933	370.603	393.366	396.847	422.673	
	(Axial /Radial)	(Axial /Radial)	(Axial)	(Radial)	(Axial /Radial)	(Axial /Radial)	

Wavelength of the lines used in ICP/AES

8. References

1. Hench, L.L. The Story of Bioglass. *J. Mater. Sci. Mater. Med.* **2006**, *17*, 967–978, doi:10.1007/s10856-006-0432-z.
2. Gritsch, L.; Perrin, E.; Chenal, J.-M.; Fredholm, Y.; Maçon, A.L.; Chevalier, J.; Boccaccini, A.R. Combining Bioresorbable Polyesters and Bioactive Glasses: Orthopedic Applications of Composite Implants and Bone Tissue Engineering Scaffolds. *Appl. Mater. Today* **2021**, *22*, 100923, doi:10.1016/j.apmt.2020.100923.
3. Välimäki, V.-V.; Aro, H.T. Molecular Basis for Action of Bioactive Glasses as Bone Graft Substitute. *Scand. J. Surg.* **2006**, *95*, 95–102, doi:10.1177/145749690609500204.
4. Singhvi, M.; Gokhale, D. Biomass to Biodegradable Polymer (PLA). *RSC Adv.* **2013**, *3*, 13558–13568, doi:10.1039/C3RA41592A.
5. Nduko, J.M.; Taguchi, S. Microbial Production of Biodegradable Lactate-Based Polymers and Oligomeric Building Blocks From Renewable and Waste Resources. *Front. Bioeng. Biotechnol.* **2021**, *8*, 1548, doi:10.3389/fbioe.2020.618077.
6. DeJong, L.E.S.; DeBerardino, L.T.M.; Brooks, D.E.; Judson, K. In Vivo Comparison of a Metal versus a Biodegradable Suture Anchor1 1Implants and Implant Instrumentation for This Project Were Provided via Material Transfer Agreement by Arthrex, Naples, Florida, U.S.A. *Arthrosc. J. Arthrosc. Relat. Surg.* **2004**, *20*, 511–516, doi:10.1016/j.arthro.2004.03.008.
7. Benicewicz, B.C.; Hopper, P.K. Review : Polymers for Absorbable Surgical Sutures—Part I. *J. Bioact. Compat. Polym.* **1990**, *5*, 453–472, doi:10.1177/088391159000500407.
8. Snežana, I.-S.; Nikolić, L.; Vesna, N.; Ilić, D.; Ristić, I.S.; Tačić, A. Polymeric Matrix Systems for Drug Delivery. In *Drug Delivery Approaches and Nanosystems*; Apple Academic Press, 2017 ISBN 978-1-315-22537-1.
9. Blaker, J.J.; Gough, J.E.; Maquet, V.; Notingher, I.; Boccaccini, A.R. In Vitro Evaluation of Novel Bioactive Composites Based on Bioglass®-Filled Polylactide Foams for Bone Tissue Engineering Scaffolds. *J. Biomed. Mater. Res. A* **2003**, *67A*, 1401–1411, doi:10.1002/jbm.a.20055.
10. Verrier, S.; Blaker, J.J.; Maquet, V.; Hench, L.L.; Boccaccini, A.R. PDLLA/Bioglass® Composites for Soft-Tissue and Hard-Tissue Engineering: An in Vitro Cell Biology Assessment. *Biomaterials* **2004**, *25*, 3013–3021, doi:10.1016/j.biomaterials.2003.09.081.
11. Blaker, J.J.; Nazhat, S.N.; Maquet, V.; Boccaccini, A.R. Long-Term in Vitro Degradation of PDLLA/Bioglass® Bone Scaffolds in Acellular Simulated Body Fluid. *Acta Biomater.* **2011**, *7*, 829–840, doi:10.1016/j.actbio.2010.09.013.

12. Maquet, V.; Boccaccini, A.R.; Pravata, L.; Notingher, I.; Jérôme, R. Preparation, Characterization, and in Vitro Degradation of Bioresorbable and Bioactive Composites Based on Bioglass®-Filled Polylactide Foams. *J. Biomed. Mater. Res. A* **2003**, *66A*, 335–346, doi:10.1002/jbm.a.10587.
13. Yang, X.B.; Webb, D.; Blaker, J.; Boccaccini, A.R.; Maquet, V.; Cooper, C.; Oreffo, R.O.C. Evaluation of Human Bone Marrow Stromal Cell Growth on Biodegradable Polymer/Bioglass® Composites. *Biochem. Biophys. Res. Commun.* **2006**, *342*, 1098–1107, doi:10.1016/j.bbrc.2006.02.021.
14. Evans, S.L.; Gregson, P.J. Composite Technology in Load-Bearing Orthopaedic Implants. *Biomaterials* **1998**, *19*, 1329–1342, doi:10.1016/S0142-9612(97)00217-2.
15. Stavropoulos, P.; Foteinopoulos, P. Modelling of Additive Manufacturing Processes: A Review and Classification. *Manuf. Rev.* **2018**, *5*, 2, doi:10.1051/mfreview/2017014.
16. Wang, X.; Jiang, M.; Zhou, Z.; Gou, J.; Hui, D. 3D Printing of Polymer Matrix Composites: A Review and Prospective. *Compos. Part B Eng.* **2017**, *110*, 442–458, doi:10.1016/j.compositesb.2016.11.034.
17. Zhang, L.; Yang, G.; Johnson, B.N.; Jia, X. Three-Dimensional (3D) Printed Scaffold and Material Selection for Bone Repair. *Acta Biomater.* **2019**, *84*, 16–33, doi:10.1016/j.actbio.2018.11.039.
18. Murariu, M.; Dubois, P. PLA Composites: From Production to Properties. *Adv. Drug Deliv. Rev.* **2016**, *107*, 17–46, doi:10.1016/j.addr.2016.04.003.
19. Guvendiren, M.; Molde, J.; Soares, R.M.D.; Kohn, J. Designing Biomaterials for 3D Printing. *ACS Biomater. Sci. Eng.* **2016**, *2*, 1679–1693, doi:10.1021/acsbiomaterials.6b00121.
20. Gregor, A.; Filová, E.; Novák, M.; Kronek, J.; Chlup, H.; Buzgo, M.; Blahnová, V.; Lukášová, V.; Bartoš, M.; Nečas, A.; et al. Designing of PLA Scaffolds for Bone Tissue Replacement Fabricated by Ordinary Commercial 3D Printer. *J. Biol. Eng.* **2017**, *11*, 31, doi:10.1186/s13036-017-0074-3.
21. Grémare, A.; Guduric, V.; Bareille, R.; Heroguez, V.; Latour, S.; L'heureux, N.; Fricain, J.-C.; Catros, S.; Le Nihouannen, D. Characterization of Printed PLA Scaffolds for Bone Tissue Engineering. *J. Biomed. Mater. Res. A* **2018**, *106*, 887–894, doi:10.1002/jbm.a.36289.
22. Engelberg, I.; Kohn, J. Physico-Mechanical Properties of Degradable Polymers Used in Medical Applications: A Comparative Study. *Biomaterials* **1991**, *12*, 292–304, doi:10.1016/0142-9612(91)90037-B.
23. Ginsac, N. Caractérisation de matériaux composite polyacide lactique-bioverre pour application dans la réparation osseuse. phdthesis, INSA de Lyon, 2011.
24. Dykman, L.A.; Khlebtsov, N.G. Gold Nanoparticles in Biology and Medicine: Recent Advances and Prospects. *Acta Naturae* **2011**, *3*, 34–55.
25. Daniel, M.-C.; Astruc, D. Gold Nanoparticles: Assembly, Supramolecular Chemistry, Quantum-Size-Related Properties, and Applications toward Biology, Catalysis, and Nanotechnology. *Chem. Rev.* **2004**, *104*, 293–346, doi:10.1021/cr030698+.

26. Hatakeyama, Y.; Onishi, K.; Nishikawa, K. Effects of Sputtering Conditions on Formation of Gold Nanoparticles in Sputter Deposition Technique. *RSC Adv.* **2011**, *1*, 1815–1821, doi:10.1039/C1RA00688F.
27. FreeCAD: Your Own 3D Parametric Modeler Available online: <https://www.freecadweb.org/> (accessed on 23 March 2022).
28. Ultimaker Cura: Powerful, Easy-to-Use 3D Printing Software Available online: <https://ultimaker.com/software/ultimaker-cura> (accessed on 12 April 2022).
29. Brossard, C.; Vlach, M.; Vène, E.; Ribault, C.; Dorcet, V.; Noiret, N.; Loyer, P.; Lepareur, N.; Cammas-Marion, S. Synthesis of Poly(Malic Acid) Derivatives End-Functionalized with Peptides and Preparation of Biocompatible Nanoparticles to Target Hepatoma Cells. *Nanomaterials* **2021**, *11*, 958, doi:10.3390/nano11040958.
30. Blond, P.; Bevernaegie, R.; Troian-Gautier, L.; Lagrost, C.; Hubert, J.; Reniers, F.; Raussens, V.; Jabin, I. Ready-to-Use Germanium Surfaces for the Development of FTIR-Based Biosensors for Proteins. *Langmuir* **2020**, *36*, 12068–12076, doi:10.1021/acs.langmuir.0c02681.
31. Mosbahi, S.; Oudadesse, H.; Roiland, C.; Lefevre, B.; Slimani, L.; Keskes, H. Risedronate Effects on the In Vivo Bioactive Glass Behavior: Nuclear Magnetic Resonance and Histopathological Studies. *BioMed Res. Int.* **2019**, *2019*, e2175731, doi:10.1155/2019/2175731.
32. Rocton, N.; Oudadesse, H.; Lefevre, B.; Peisker, H.; Rbii, K. Fine Analysis of Interaction Mechanism of Bioactive Glass Surface after Soaking in SBF Solution: AFM and ICP-OES Investigations. *Appl. Surf. Sci.* **2020**, *505*, 144076, doi:10.1016/j.apsusc.2019.144076.
33. Puppi, D.; Chiellini, F.; Piras, A.M.; Chiellini, E. Polymeric Materials for Bone and Cartilage Repair. *Prog. Polym. Sci.* **2010**, *35*, 403–440, doi:10.1016/j.progpolymsci.2010.01.006.
34. Chacón, J.M.; Caminero, M.A.; García-Plaza, E.; Núñez, P.J. Additive Manufacturing of PLA Structures Using Fused Deposition Modelling: Effect of Process Parameters on Mechanical Properties and Their Optimal Selection. *Mater. Des.* **2017**, *124*, 143–157, doi:10.1016/j.matdes.2017.03.065.
35. Kong, L.; Gao, Y.; Lu, G.; Gong, Y.; Zhao, N.; Zhang, X. A Study on the Bioactivity of Chitosan/Nano-Hydroxyapatite Composite Scaffolds for Bone Tissue Engineering. *Eur. Polym. J.* **2006**, *42*, 3171–3179, doi:10.1016/j.eurpolymj.2006.08.009.
36. Hupa, L.; Karlsson, K.H.; Hupa, M.; Aro, H.T. Comparison of Bioactive Glasses in Vitro and in Vivo. *Glass Technol. - Eur. J. Glass Sci. Technol. Part A* **2010**, *51*, 89–92.
37. Vallittu, P.K.; Posti, J.P.; Piitulainen, J.M.; Serlo, W.; Määttä, J.A.; Heino, T.J.; Pagliari, S.; Syrjänen, S.M.; Forte, G. Biomaterial and Implant Induced Ossification: In Vitro and in Vivo Findings. *J. Tissue Eng. Regen. Med.* **2020**, *14*, 1157–1168, doi:10.1002/term.3056.

38. Rocton, N.; Oudadesse, H.; Lefeuve, B.; Peisker, H.; Rbii, K. Fine Analysis of Interaction Mechanism of Bioactive Glass Surface after Soaking in SBF Solution: AFM and ICP-OES Investigations. *Appl. Surf. Sci.* **2020**, *505*, 144076, doi:10.1016/j.apsusc.2019.144076.

Journal Pre-proof